DALTON

Synthesis and structural characterization of [$PtCl_2$\{*meso*-Ph(HO)PCH_2-CH_2P(OH)Ph\}] and structurally related derivatives

John Powell,* Michael J. Horvath and Alan Lough

Department of Chemistry, University of Toronto, Toronto, M5S 1A1, Canada

The compound *meso*-PhH(O)PCH_2CH_2P(O)HPh reacted with [$PtCl_2$(cod)] (cod = cycloocta-1,5-diene) and 2NaOMe to give the tetramer complex [\{Pt[(*R,S*)-Ph(O)PCH_2CH_2P(O)Ph]\}$_4$]. Treatment of the latter with HCl gave [$PtCl_2$\{(*R,S*)-Ph(HO)PCH_2CH_2P(OH)Ph\}] in high yield. This complex with PPh_3 gave [PtCl(PPh_3)\{(*R,S*)-Ph(HO)PCH_2CH_2P(OH)Ph\}]Cl which can be readily deprotonated to [PtCl(PPh_3)\{(*R,S*)-Ph(O)PCH_2CH_2P(OH)Ph\}] which exists in solution in two isomeric forms [P(OH)Ph group *cis* or *trans* to Cl]. Treatment of *trans*-[PtCl(COR)$(PPh_3)_2$] (R = Me or Ph) with *meso*-PhH(O)PCH_2CH_2P(O)HPh gave the cationic complexes [Pt(COR)(PPh_3)\{(*R,S*)-Ph(HO)PCH_2CH_2P(OH)Ph\}]Cl (R = Me or Ph). These complexes are moisture sensitive and react readily with water. The molecular structures of three complexes have been determined by single-crystal X-ray diffraction.

Secondary phosphine oxides $R_2P(O)H$ and their phosphinous acid tautomers R_2POH constitute a simple class of ditopic compounds capable of bonding to transition metals through both 'soft' phosphorus and 'hard' oxygen donor atoms.[1] However, the ligating properties of the phosphinous acid tautomer towards the later transition metals of the second and third row is limited to some degree by the fact that free R_2POH rapidly equilibrates with the more weakly ligating secondary phosphine oxide $R_2P(O)H$ which is the more stable tautomeric form.[1,2] A means of overcoming this problem involves the application of the chelate effect to increase the stability of phosphinous acid complexes[3] and we have recently described a range of bis-chelated platinum(II) complexes derived from the reaction of [$Pt(PPh_3)_4$] with either the *meso* or racemic form of PhH(O)PCH_2CH_2P(O)HPh (*e.g.* complex **1** in Scheme 1).[4] However, complexes of this type clearly have a limited potential for structural diversity and reaction chemistry because the two chelating ligands occupy the available four co-ordination sites at Pt^{II}. An obvious solution to this problem was to synthesize complexes incorporating only one *meso*/*rac* ligand per platinum(II) centre. In this paper we describe the synthesis and characterization of the useful starting precursor complex [$PtCl_2$\{*meso*-Ph(HO)PCH_2CH_2P(OH)Ph\}] and structurally related derivatives.

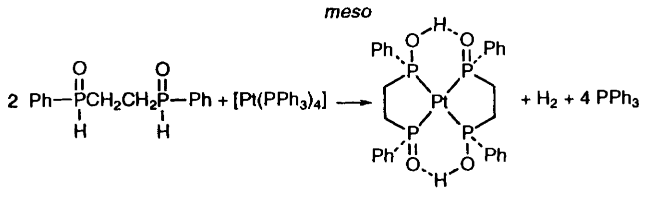

1

Scheme 1

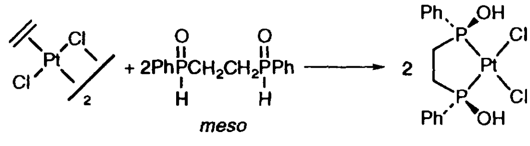

2, low yield 20–30%

Scheme 2

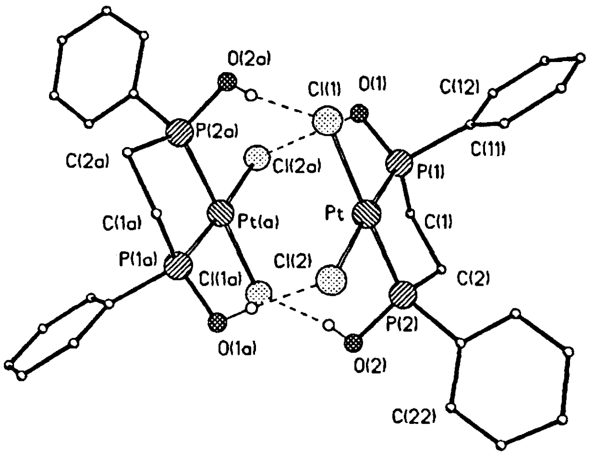

Fig. 1 Molecular structure of the complex [$PtCl_2$\{(*R,S*)-Ph(HO)-PCH_2CH_2P(OH)Ph\}] **2**

Results and Discussion

Our initial method for preparing the complex [$PtCl_2$\{(*R,S*)-Ph(HO)PCH_2CH_2P(OH)Ph\}] **2** involved treating Zeise's dimer with 2 equivalents of *meso*-(*R,S*)-PhH(O)PCH_2CH_2P(O)HPh (Scheme 2). On work-up **2** was isolated in yields of 20–30%. The poor yield originated from competing side reactions giving the previously reported bis-chelate complexes *syn*-[Pt\{*R,S*-Ph(O)PCH_2CH_2P(OH)Ph\}\{*R,S*-Ph(HO)PCH_2CH_2P(OH)Ph\}]Cl and *anti*-[Pt\{*R,S*-Ph(HO)PCH_2CH_2P(OH)Ph\}$_2$]-Cl_2.[4] Complex **2** was characterized by its ^{31}P-\{^1H\} NMR and mass spectral data, and its molecular structure determined from a single-crystal X-ray diffraction study. The ^{31}P-\{^1H\} NMR spectrum exhibits a singlet resonance at δ 104.5 with a large ^{195}Pt–^{31}P coupling constant of 4097 Hz consistent with two equivalent phosphorus donor atoms each *trans* to a low-*trans*-influence chloride.[5] The mass spectrum exhibited an ion fragment at *m*/*z* 1051 consistent with a [dimer − Cl]$^+$ ion. A dimeric structural arrangement was confirmed by single-crystal X-ray diffraction. The molecular structure is shown in Fig. 1 and selected bond lengths and angles are given in Table 1. In the solid state, molecules of **2** stack as dimers *via* intermolecular OH···Cl hydrogen bonds (Cl···O 2.974–3.002 Å). Each molecule contains a platinum atom bonded to two chloride atoms and chelated by a *meso*-(*R,S*)-Ph(HO)PCH_2CH_2-

P(OH)Ph ligand. The short Pt–P distances of 2.205(2) to 2.207(2) Å reflect the low *trans* influence of the chloride atoms.[5]

In order to obtain complex **2** in higher yield the chelation of a second *meso* ligand to Pt^{II} must be suppressed. Our first attempt towards this end involved preparing the acetate-bridged dimer $[\{Pt(MeCO_2C_8H_{12})(O_2CMe\}_2]$ **3** *in situ* by the reaction of $[PtCl_2(cod)]$ (cod = cycloocta-1,5-diene) with AgO_2CMe[6] and treating it with 1 equivalent of the *meso* ligand per Pt. In doing so, it was conceived that the desired intermediate complex $[Pt\{R,S\text{-}Ph(HO)PCH_2CH_2P(OH)Ph\}(MeCO_2C_8H_{12})][O_2CMe]$ **4** would be obtained in which the $MeCO_2C_8H_{12}$ ligand was still bound to the platinum(II) centre. Treatment of this complex with HCl would presumably yield the desired dichloroplatinum(II) complex **2** together with free $MeCO_2C_8H_{13}$. Using this method **2** was isolated in 64% yield. However, monitoring the reaction by $^{31}P\text{-}\{^1H\}$ NMR spectroscopy showed that the intermediate complex formed was not the expected species **4**. After filtration of the reaction mixture to remove AgCl and prior to reaction with HCl the yellow filtrate was analysed by its $^{31}P\text{-}\{^1H\}$ NMR spectrum. A major signal was observed at δ 94.5 $[J(^{195}Pt\text{-}^{31}P) = 4340$ Hz] together with a minor signal at δ 80.6 $[J(^{195}Pt\text{-}^{31}P) = 4340$ Hz] and a very broad signal at δ 50. The signals at δ 80.6 and 94.5 exhibit large $^{195}Pt\text{-}^{31}P$ coupling constants consistent with complexes containing P donors *trans* to low-*trans*-influence oxygen-donor atoms about Pt^{II}.[5] These signals do not originate from the anticipated intermediate **4** which would give rise to a complex $^{31}P\text{-}\{^1H\}$ NMR spectrum based on the asymmetry in the molecule. Treatment of the reaction solution with dry HCl resulted in the disappearance of the signals at δ 80.6 and 94.5 and the appearance of a singlet at δ 104.6 $[J(^{195}Pt\text{-}^{31}P) = 4098$ Hz] originating from the dichloro complex **2** together with a very broad and unidentified signal at δ 80. The major intermediate giving rise to the signal at δ 94.5 is identified as the tetrameric complex $[\{Pt[(R,S)\text{-}Ph(O)PCH_2CH_2P(O)Ph]\}_4]$ **5** based on the following experiments. Treatment of $[PtCl_2(cod)]$ with 2 equivalents of NaOMe in MeOH followed by addition of 1 equivalent of the *meso* ligand $(R,S)\text{-}PhH(O)PCH_2CH_2P(O)HPh$ yielded the tetrameric complex **5** as a white crystalline product in 75% yield (Scheme 3). Addition of dry HCl to a solution of **5** in CH_2Cl_2 afforded complex **2** in nearly quantitative yield.

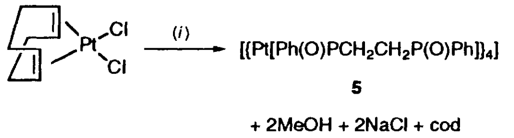

Scheme 3 (*i*) 2NaOMe in MeOH, *meso*-$PhH(O)PCH_2CH_2P(O)HPh$

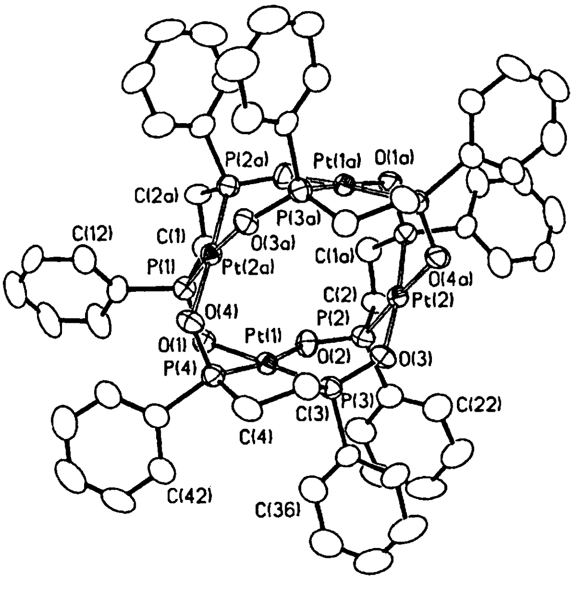

Fig. 2 Molecular structure of the complex $[\{Pt[(R,S)\text{-}Ph(O)PCH_2CH_2P(O)Ph]\}_4]\cdot 7CH_2Cl_2$ **5**

Table 1 Selected bond lengths (Å) and angles (°) for $[PtCl_2\{(R,S)\text{-}Ph(HO)PCH_2CH_2P(OH)Ph\}]$ **2**

Pt–P(1)	2.207(2)	O(1)–H(1o)	0.850
Pt–P(2)	2.205(2)	O(2)–H(2o)	0.850
Pt–Cl(1)	2.380(2)	H(1o) ··· Cl(2a)	2.24
Pt–Cl(2)	2.382(2)	H(2o) ··· Cl(1a)	2.17
P(1)–O(1)	1.577(7)	O(1) ··· Cl(2a)	3.031(6)
P(2)–O(2)	1.578(5)	O(2) ··· Cl(1a)	3.017(6)
P(1)–Pt–P(2)	87.1(1)	Pt–P(1)–O(1)	119.8(2)
Cl(1)–Pt–Cl(2)	89.8(1)	Pt–P(2)–O(2)	116.3(3)
Cl(2)–Pt–P(1)	93.6(1)	P(1)–O(1)–H(1o)	115.2
Cl(1)–Pt–P(2)	89.4(1)	P(2)–O(2)–H(2o)	112.5
Cl(1)–Pt–P(1)	176.3(1)	O(1)–H(1o) ··· Cl(1a)	154
Cl(2)–Pt–P(2)	177.4(1)	O(2)–H(2o) ··· Cl(2a)	173

Complex **5** was characterized by ^1H and $^{31}P\text{-}\{^1H\}$ NMR spectroscopy as well as by mass spectrometry and microanalyses. Its tetrameric nature was suggested by the observation of an intense parent-ion peak at *m*/*z* 1885 in the mass spectrum, and confirmed by single-crystal X-ray diffraction. The molecular structure is shown in Fig. 2 and selected bond lengths and angles are given in Table 2. The complex is a cyclic tetramer constructed from four Pt atoms and four bis-phosphinito *meso* ligands $(R,S)\text{-}Ph(O)PCH_2CH_2P(O)Ph$. Notably, the lattice contains seven molecules of CH_2Cl_2 per molecule of **5**. Each Pt atom is chelated by a *meso* ligand through phosphorus and *cis* bonded to two phosphoryl oxygen atoms (P=O) originating from separate *meso* ligands in an approximately square-planar co-ordination geometry. Bridging P=O groups link the $Pt\{(R,S)\text{-}Ph(O)PCH_2CH_2P(O)Ph\}$ subunits together in a zigzag fashion to give the cyclic tetramer structure. The ability of a P=O group to bridge two Pt atoms has been previously observed. Examples include the diplatinum(I) complexes $[Pt_2(\mu\text{-}OPPh_2)_2(PR_3)_2]$ **6** (R_3 = $MePh_2$ or Ph_3) and the triplatinum(II) complexes $[Pt_3(\mu_3\text{-}OH)(\mu\text{-}OPPh_2)_3(PR_3)_3]^{2+}$ **7** (R_3 = $MePh_2$ or Ph_3) prepared by Orpen and co-workers.[7] The relatively short Pt–P distances, which vary from 2.200(3) to

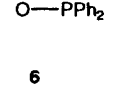

6

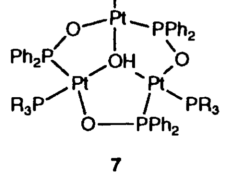

7

Table 2 Selected bond lengths (Å) and angles (°) for $[\{Pt[(R,S)\text{-}Ph(O)PCH_2CH_2P(O)Ph]\}_4]\cdot 7CH_2Cl_2$ **5**

Pt(1)–P(3)	2.209(3)	Pt(2a)–O(4)	2.135(7)
Pt(1)–P(4)	2.202(3)	P(1)–O(1)	1.548(9)
Pt(1)–P(2a)	2.206(3)	P(2)–O(2)	1.537(7)
Pt(2)–P(2)	2.200(3)	P(3)–O(3)	1.545(7)
Pt(2)–P(1a)	2.206(3)	P(4)–O(4)	1.539(10)
Pt(1)–O(1)	2.146(7)	Pt(1) ··· Pt(1a)	5.124(3)
Pt(1)–O(2)	2.114(7)	Pt(1) ··· Pt(2a)	3.335(3)
Pt(2)–O(3)	2.103(7)	Pt(1) ··· Pt(2)	3.852(3)
Pt(2)–O(4a)	2.135(7)	Pt(2) ··· Pt(2a)	5.065(3)
P(3)–Pt(1)–P(4)	86.2(1)	P(1a)–Pt(2)–O(3)	174.6(2)
P(2)–Pt(2)–P(1a)	86.6(1)	P(1a)–Pt(2)–O(4a)	94.8(2)
P(3)–Pt(1)–O(1)	175.4(2)	P(2)–Pt(2)–O(4a)	177.0(3)
P(3)–Pt(1)–O(2)	101.3(2)	O(1)–Pt(1)–O(2)	83.2(3)
P(4)–Pt(1)–O(2)	170.8(2)	O(3)–Pt(2)–O(4a)	85.7(3)
P(4)–Pt(1)–O(1)	89.2(2)		

Table 3 ^{31}P-{^{1}H} NMR data (δ, J/Hz) for complexes **8**, **9a**, **9b**, **10** and **11** in CH_2Cl_2

Complex	X	$\delta(P_L)$	$\delta(P_A)$	$\delta(P_B)$	$J(Pt-P_L)$	$J(Pt-P_A)$	$J(Pt-P_B)$	$J(P_A-P_L)$	$J(P_B-P_L)$
8	Cl	22.9	104.0	122.2	2282	3905	2869	19	416
9a[a]		24.8	86.4	108.6	2134	3852	3017	18	415
9b[b]		24.75	87.2	108.2	2090	3842	3024	18	420
10	MeCO	15.6	118.5	114.9	2859	1626	3412	26	337
11	PhCO	16.6	118.8	114.0	2784	1694	3329	25	343

[a] $J(P_A-P_B)$ 4.0 Hz. [b] $J(P_A-P_B)$ 4.5 Hz.

2.209(3) Å, reflect the low *trans* influence of the phosphoryl oxygen donor atoms. Close Pt···Pt non-bonding contacts [Pt(1)···Pt(2) and Pt(1)···Pt(2a)] are 3.852 and 3.335 Å and the long Pt···Pt non-bonding contacts [Pt(1)···Pt(1A) and Pt(2)···Pt(2a)] are 5.124 and 5.065 Å. (A consideration of the long Pt···Pt distances suggests the possibility of incorporating suitably sized cations/anions into the interior of the Pt_4 framework.) The solution ^{31}P-{^{1}H} NMR spectrum of **5** in CH_2Cl_2 exhibits a signal centred at δ 94.5 [$^{1}J(^{195}Pt-^{31}P)$ = 4340, $^{2}J(^{195}Pt-^{31}P)$ = 47 Hz] consistent with the molecular structure in that each of the eight chemically equivalent phosphorus atoms has the opportunity to couple with two magnetically different Pt atoms. While the large $^{1}J(^{195}Pt-^{31}P)$ coupling originates from P bonded to Pt, the longer range $^{2}J(^{195}Pt-^{31}P)$ probably originates *via* the P=O bridge. This type of spin system involving a P=O bridge between two chemically equivalent Pt atoms has been previously observed for complexes **6** and **7**.[7]

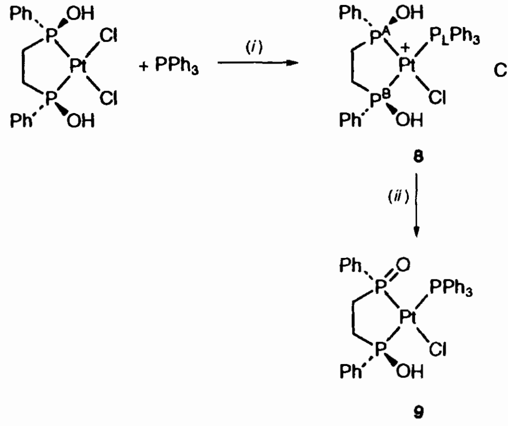

Scheme 4 (*i*) CH_2Cl_2; (*ii*) NaOMe

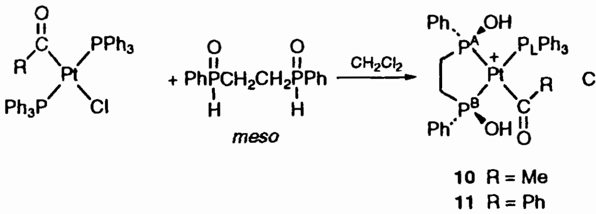

Scheme 5

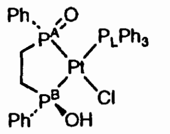

9a

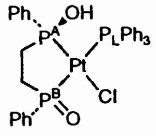

9b

Preparation and spectroscopic characterization of complexes 8 and 9

The reaction of complex **2** with 1 equivalent of PPh_3 affords the cationic complex [PtCl(PPh_3){(*R*,*S*)-Ph(HO)PCH_2CH_2-P(OH)Ph}]Cl **8** in 87% yield (Scheme 4). Complex **8** is deprotonated by NaOMe in CH_2Cl_2 (trace MeOH) to give the neutral complex [PtCl(PPh_3){(*R*,*S*)-Ph(O)PCH_2CH_2-P(OH)Ph}] **9** in an overall yield of 90% (Scheme 4). Both complexes **8** and **9** are characterized by their ^{31}P-{^{1}H} NMR (Table 3) and mass spectral data. Notably, the ^{31}P-{^{1}H} NMR spectrum of the neutral complex **9** recorded in dry CH_2Cl_2 exhibits signals which are consistent with the presence of the isomeric species **9a** and **9b** in *ca.* 53 : 47 ratio. While the two isomers differ only in respect of the disposition of the P–OH and P=O groups relative to the remaining ligands, an unambiguous assignment of the ^{31}P-{^{1}H} NMR signal sets to isomers **9a** and **9b** is not possible on the basis of these data. Under conditions of 'wet' CH_2Cl_2 (*i.e.* one drop of water added) the ^{31}P-{^{1}H} signals of **9a** and **9b** collapse to give broad signals in the region of the *meso* ligand at δ 86.8 and 108.8, and only a single doublet of doublets pattern centred at δ 24.8 in the co-ordinated PPh_3 region (coupling to ^{195}Pt still observed). These results indicate a water-assisted fast proton exchange between the phosphoryl oxygen atoms of the *meso* ligand in complex **9** with the result being a 'time-averaged' ^{31}P-{^{1}H} NMR spectrum. In the absence of water, the proton exchange either does not occur or is sufficiently slow that isomers **9a** and **9b** are spectroscopically observed.

Preparation, structural analysis, and reactivity of acyl complexes 10 and 11

The above studies illustrate that under appropriate conditions (*i.e.* complete deprotonation of the *meso* ligand) formation of platinum(II) bis-chelate complexes is suppressed and a number of platinum(II) mono-chelate complexes have been prepared. The formation of the bis-chelate complexes can also be suppressed by incorporating substitutionally inert acyl ligands into the platinum(II) starting materials. Thus the acyl complexes *trans*-[PtCl(COR)(PPh_3)$_2$] react with the *meso* ligand (*R*,*S*)-PhH(O)PCH_2CH_2P(O)HPh to afford the cationic platinum(II) acyl complexes [Pt(COR)(PPh_3){(*R*,*S*)-Ph(HO)PCH_2CH_2-P(OH)Ph}]Cl [R = Me **10** or Ph **11** (Scheme 5)]. Both **10** and **11** have been characterized by ^{31}P-{^{1}H} NMR spectroscopy (Table 3) as well as by elemental analyses and mass spectrometry. The ^{31}P-{^{1}H} NMR spectrum of complex **10** consists of three resonances originating from P_A, P_B and PPh_3. The upfield doublet of doublets at δ 15.6 is assigned to the PPh_3 ligand *trans* to P_B and *cis* to P_A [$^{2}J(^{31}P-^{31}P)$ = 337.26 Hz]. Atom P_B gives rise to a broad doublet at δ 114.9 ($w_{\frac{1}{2}}$ = 47 Hz) exhibiting *trans* coupling to PPh_3 [$^{2}J(^{31}P-^{31}P)$ = 337 Hz] and a relatively large coupling to Pt [$J(^{195}Pt-^{31}P_B)$ = 3412 Hz]. The broadness of this signal may be a result of a fast H^+ exchange between the phosphoryl oxygen and the neighbouring acetyl oxygen. The doublet at δ 118.5 is assigned to P_A and exhibits coupling to Pt and PPh_3 [$^{2}J(^{31}P_A-^{31}P_L)$ = 26, $J(^{195}Pt-^{31}P_A)$ = 1626 Hz]. The small $J(^{195}Pt-^{31}P_A)$ value is consistent with P_A *trans* to acetyl (COMe), a group of high *trans* influence.[5] The ^{31}P-{^{1}H} NMR spectrum of complex **11** exhibits analogous features to those of **10**.

The molecular structure of complex **10** as determined by single-crystal X-ray diffraction is shown in Fig. 3. Bond lengths

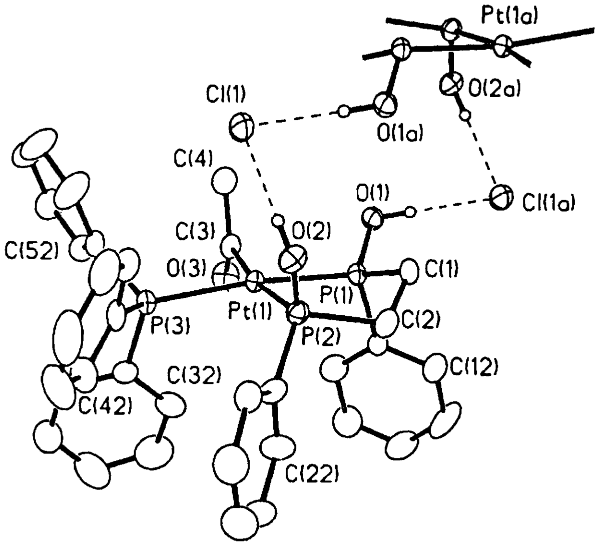

Fig. 3 Molecular structure of the complex [Pt(COMe)(PPh$_3$){(*R*,*S*)-Ph(HO)PCH$_2$CH$_2$P(OH)Ph}]Cl **10**

Table 4 Selected bond lengths (Å) and angles (°) for [Pt(COMe)(PPh$_3$){(*R*,*S*)-Ph(HO)P(CH$_2$)$_2$P(OH)Ph}]Cl **10**

Pt(1)–P(1)	2.271(2)	P(1)–O(1)	1.585(8)
Pt(1)–P(2)	2.322(3)	P(2)–O(2)	1.578(6)
Pt(1)–P(3)	2.338(2)	Cl(1)···O(2)	2.997(5)
Pt(1)–C(3)	2.098(10)	Cl(1a)···O(1)	2.928(5)
O(3)–C(3)	1.152(12)	H(1o)–Cl(1a)	2.08
C(3)–C(4)	1.470(15)	H(2o)–Cl(1)	2.15
P(1)–Pt(1)–P(2)	84.2(1)	P(3)–Pt(1)–C(3)	88.0(3)
P(2)–Pt(1)–P(3)	99.2(1)	Pt(1)–C(3)–O(3)	122.0(8)
P(1)–Pt(1)–P(3)	171.0(1)	Pt(1)–C(3)–C(4)	114.6(7)
P(1)–Pt(1)–C(3)	89.4(2)	O(3)–C(3)–C(4)	123.3(11)
P(2)–Pt(1)–C(3)	171.4(2)		

and angles are given in Table 4. In the solid state, molecules of **10** exist as dimers *via* OH ··· Cl$^-$ ··· HO bonding interactions [Cl$^-$ ··· O distances 2.928(5) to 2.997(5) Å]. This situation however precludes any interaction between the acetyl oxygen and the *cis*-OH group. Each molecule of **10** contains a platinum atom bonded to PPh$_3$ and an acetyl group as well as chelated to an (*R*,*S*)-Ph(OH)PCH$_2$CH$_2$P(OH)Ph ligand. The co-ordination geometry about each platinum atom is approximately square planar. Notably, the Pt(1)–P(2) distance of 2.322(3) Å is significantly longer (0.051 Å) than the Pt(1)–P(1) distance of 2.271(2) Å. This difference in Pt–P bond lengths reflects the greater *trans* influence of the COMe group [*trans* to P(2)] compared to that of PPh$_3$ [*trans* to P(1)].[5]

Hydrolysis of complex 10

During the synthesis of complexes **10** and **11** it was observed that they were sensitive to water. Monitoring of the reaction of water with the cationic complex **10** in CH$_2$Cl$_2$ by ^{31}P-{^{1}H} NMR showed, after 23 h, the formation of **9** as the major product together with a small amount (< 5%) of unreacted **10** (Scheme 6). Acetic acid was detected by ^{1}H NMR spectroscopy. Interestingly when 1 equivalent of PPh$_3$ was added to a solution containing **10** prior to the addition of water the hydrolysis reaction was dramatically impeded. After 21 h a ^{31}P-{^{1}H} NMR spectrum of the solution showed that 80% of the cationic complex **10** remained. While the major product was the platinum(II) bis-chelate complex **1** (12% yield), minor amounts of the neutral chloride complex **9** (6% yield) and the cationic chloride complex **8** (2% yield) were also observed. These observations *suggest* that the presence of PPh$_3$ inhibits a pre-equilibrium dissociation of PPh$_3$ from **10**, a step necessary for the hydrolysis reaction to occur. Whether or not the vacant site generated by this dissociation is then occupied by H$_2$O or perhaps the acyl oxygen to afford an η^2-acyl complex has not yet been discerned.

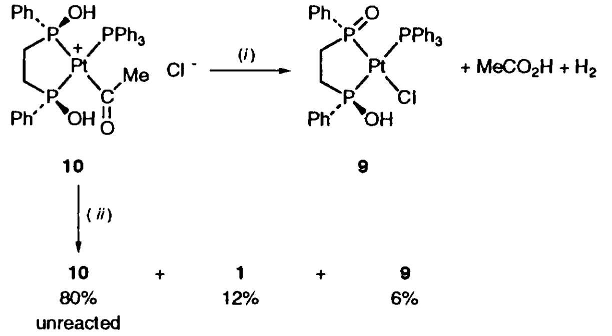

Scheme 6 (*i*) Water; (*ii*) water, PPh$_3$

Experimental

Starting materials

1,2-Bis(diphenylphosphino)ethane and K$_2$[PtCl$_4$] were obtained from Digital Specialty Chemicals Inc. The ligand *meso*-PhH(O)PCH$_2$CH$_2$P(O)HPh[4] and [PtCl$_2$(cod)][8] were prepared according to literature methods. The ^{31}P-{^{1}H} NMR spectra were recorded on a Varian Gemini-300 MHz spectrometer and referenced to 85% H$_3$PO$_4$. Microanalyses were carried out by Canadian Microanalytical Laboratories.

Preparations

[{Pt[(*R*,*S*)-Ph(O)PCH$_2$CH$_2$P(O)Ph]}$_4$] 5. To a stirred pale yellow suspension of [PtCl$_2$(cod)] (0.219 g, 0.588 mmol) in MeOH (15 cm^3) was added NaOMe (0.066 g, 1.22 mmol). The resultant white mixture was stirred whilst adding *meso*-PhH(O)PCH$_2$CH$_2$P(O)HPh (0.164 g, 0.589 mmol) over 2 min to give a colourless solution. After 10 min a white precipitate began to form. The mixture was left to stand overnight and then the white solid collected on a sintered glass frit, washed with diethyl ether and dried. It was extracted with CH$_2$Cl$_2$ (3 × 20 cm^3) and the combined filtered extracts evaporated to dryness to afford complex **5** as a white solid (yield 0.21 g, 75%), m.p. 290–320 °C (Found: C, 35.70; H, 3.00. Calc. for C$_{14}$H$_{14}$O$_2$P$_2$Pt: C, 36.65; H, 3.10%). ^{31}P-{^{1}H} NMR (CH$_2$Cl$_2$): δ 94.5 [^1J(^{195}Pt–^{31}P) = 4340, ^2J(^{195}Pt–^{31}P) = 47 Hz].

Crystals suitable for a single-crystal X-ray diffraction study were obtained from CH$_2$Cl$_2$–diethyl ether.

[PtCl$_2${(*R*,*S*)-Ph(HO)PCH$_2$CH$_2$P(OH)Ph}] 2. Hydrogen chloride was slowly bubbled through a colourless CH$_2$Cl$_2$ solution containing [{Pt[(*R*,*S*)-Ph(O)PCH$_2$CH$_2$P(O)Ph]}$_4$] **5** (0.061 g) for 15 min. The resultant white mixture was concentrated to dryness to afford complex **2** as a white solid (yield 0.067 g, 95%). Mass spectrum (FAB, 3-nitrobenzyl alcohol matrix): *m*/*z* 1051, [{PtCl$_2$[(*R*,*S*)-Ph(HO)PCH$_2$CH$_2$P(OH)Ph]}$_2$ − Cl$^-$]$^+$; 509, [PtCl{(*R*,*S*)-Ph(HO)PCH$_2$CH$_2$P(OH)Ph}]$^+$ (monomer ion − Cl) (Found: C, 30.80; H, 2.95. Calc. for C$_{14}$H$_{16}$Cl$_2$O$_2$P$_2$Pt: C, 30.90; H, 2.95%). Crystals suitable for a single-crystal X-ray diffraction study were obtained from CH$_2$Cl$_2$.

[PtCl(PPh$_3$){(*R*,*S*)-Ph(HO)PCH$_2$CH$_2$P(OH)Ph}]Cl 8. To a stirred white mixture containing [PtCl$_2${(*R*,*S*)-Ph(HO)PCH$_2$CH$_2$P(OH)Ph}] **2** (0.139 g, 0.257 mmol) in CH$_2$Cl$_2$ (6 cm^3) was added PPh$_3$ (0.068 g, 0.259 mmol). The resultant slightly turbid colourless solution was stirred for 4 h and then concentrated to

Table 5 Crystallographic data for complexes **2**, **5** and **10**

	2	**5**	**10**
Empirical formula	$C_{14}H_{16}Cl_2O_2P_2Pt$	$C_{63}H_{70}Cl_{14}O_8P_8Pt_4$	$C_{34}H_{34}ClO_3P_3Pt$
M	544.2	2479.6	814.1
Crystal size/mm	0.26 × 0.14 × 0.18	0.35 × 0.15 × 0.14	0.2 × 0.2 × 0.05
Crystal class	Monoclinic	Monoclinic	Triclinic
Space group	$P2_1/c$	$C2/c$	$P\bar{1}$
a/Å	10.368(2)	21.968(4)	11.101(2)
b/Å	15.642(3)	19.348(3)	11.387(3)
c/Å	11.887(2)	20.013(4)	14.410(3)
α/°			91.20(2)
β/°	115.81(3)	104.71(2)	92.75(1)
γ/°			112.03(2)
U/Å^3	1735.4(8)	8228(3)	1685.1(7)
Z	4	4	2
D_c/g cm^{-3}	2.083	2.002	1.604
F(000)	1032	4728	804
Collection temperature/K	294	210	294
2θ range/°	2.6–50	4.0–56	5.0–50
h,k,l ranges	−14 to 12, 0–18, 0–12	0–28, 0–25, −25 to 25	−13 to 12, 0–13, −17 to 17
Reflections collected	3434	10 213	6332
Unique reflections	3051	9676	5656
Observed reflections	2206 [$F > 4.0\sigma(F)$]	5157 [$F > 4.0\sigma(F)$]	4470 [$F > 6.0\sigma(F)$]
Weighting scheme	$\sigma^2(F) + 0.0002F^2$	$\sigma^2(F) + 0.0003F^2$	$\sigma^2(F) + 0.0007F^2$
R	0.030	0.048	0.042
wR	0.029	0.045	0.056
Goodness of fit	1.02	1.28	1.49
Largest Δ/σ	0.00	0.04	0.20
$\Delta\rho_{max}$, $\Delta\rho_{min}$/e Å^{-3}	0.59, −0.68	1.01, −1.33	1.64, −0.97

2 cm^3. Slow addition of ether (3 cm^3) resulted in precipitation of a white solid. After decanting the mother-liquor the white solid **8** was washed with ether (2 × 10 cm^3) and dried *in vacuo* for 1 h (yield 0.181 g, 87%). Mass spectrum (FAB): *m/z* 771, $[\mathrm{PtCl(PPh_3)}\{(R,S)\text{-}\mathrm{Ph(HO)PCH_2CH_2P(OH)Ph}\}]^+$ (calc.: 771).

$[\mathrm{PtCl(PPh_3)}\{(R,S)\text{-}\mathrm{Ph(O)PCH_2CH_2P(OH)Ph}\}]$ 9. To a stirred solution containing $[\mathrm{PtCl(PPh_3)}\{(R,S)\text{-}\mathrm{Ph(HO)PCH_2CH_2P(OH)Ph}\}]\mathrm{Cl}$ **8** (0.117 g, 0.146 mmol) in CH_2Cl_2 (5cm^3) was added NaOMe (0.009 g, 0.16 mmol) and MeOH (*ca.* 0.2 cm^3). The resultant mixture was stirred overnight and then filtered to afford a clear and colourless filtrate. After concentrating the solution to dryness the white residue was taken up in CH_2Cl_2 (2 cm^3), and ether (2 cm^3) slowly added. The white precipitate of complex **9** which formed was washed with ether and dried *in vacuo* for 2 h (yield 0.103 g, 90%). Mass spectrum (FAB): *m/z* 771, [M + H$^+$] (calc.: 770); 734, [M^+ − HCl].

$[\mathrm{Pt(COPh)(PPh_3)}\{(R,S)\text{-}\mathrm{Ph(HO)PCH_2CH_2P(OH)Ph}\}]\mathrm{Cl}$ 11. Addition of CH_2Cl_2 (12 cm^3) to a solid mixture of *trans*-$[\mathrm{PtCl(COPh)(PPh_3)_2}]$ (0.457 g, 0.531 mmol) and *meso*-(*R*,*S*)-$\mathrm{PhH(O)PCH_2CH_2P(O)HPh}$ (0.148 g, 0.532 mmol) resulted in a clear pale yellow-green solution. After 1 h the solution was concentrated *in vacuo* to 3–4 cm^3 and ether (8 cm^3) slowly added to initiate crystallization. The resultant mixture was left to stand for 2 h. The yellow crystals of complex **11** which formed were separated from the mother-liquor, washed with ether (2 × 5 cm^3), and dried *in vacuo* for 2 h (yield 0.364 g, 78%) (Found: C, 53.15; H, 4.20. Calc. for $C_{39}H_{36}ClO_3P_3Pt$: C, 53.45; H, 4.15%). Mass spectrum (FAB): *m/z* 840, of parent ion $[\mathrm{Pt(COPh)(PPh_3)}\{(R,S)\text{-}\mathrm{Ph(HO)PCH_2CH_2P(OH)Ph}\}]^+$ (calc.: 840).

Similarly prepared was $[\mathrm{Pt(COMe)(PPh_3)}\{(R,S)\text{-}\mathrm{Ph(HO)PCH_2CH_2P(OH)Ph}\}]\mathrm{Cl}$ **10**, isolated as pale yellow crystals (yield 81%) (Found: C, 49.60; H, 4.15. Calc. for $C_{34}H_{34}ClO_3P_3Pt$: C, 50.15; H, 4.20%). Mass spectrum (FAB): *m/z* 778, $[\mathrm{Pt(COMe)(PPh_3)}\{(R,S)\text{-}\mathrm{Ph(HO)PCH_2CH_2P(OH)Ph}\}]^+$ (calc.: 779). Crystals suitable for a single-crystal X-ray diffraction study were obtained from CH_2Cl_2–ether.

Table 6 Atomic coordinates (× 10^4) of complex **2**

Atom	x	y	z
Pt	5 375(1)	9 919(1)	1 727(1)
Cl(1)	4 055(2)	11 134(1)	1 842(2)
Cl(2)	7 420(2)	10 804(1)	2 213(2)
P(1)	6 504(2)	8 741(1)	1 645(2)
P(2)	3 498(2)	9 106(1)	1 366(2)
O(1)	7 530(5)	8 755(3)	981(5)
O(2)	2 114(5)	9 290(4)	118(5)
C(1)	5 159(8)	7 936(5)	876(8)
C(2)	4 006(8)	7 993(5)	1 366(8)
C(11)	7 701(8)	8 337(5)	3 165(7)
C(12)	7 889(9)	8 763(5)	4 238(7)
C(13)	8 860(10)	8 452(6)	5 381(8)
C(14)	9 633(9)	7 735(6)	5 461(9)
C(15)	9 443(10)	7 294(6)	4 389(9)
C(16)	8 497(9)	7 607(6)	3 251(9)
C(21)	2 795(8)	9 183(5)	2 506(8)
C(22)	3 728(9)	9 049(6)	3 756(8)
C(23)	3 231(12)	9 074(6)	4 652(9)
C(24)	1 802(11)	9 236(6)	4 317(9)
C(25)	897(10)	9 376(6)	3 079(10)
C(26)	1 372(9)	9 355(5)	2 165(8)

^{31}P-{^{1}H} NMR spectroscopic studies of the hydrolysis of complex 10

To a pale yellow solution containing complex **10** (0.135 g, 0.166 mmol) in CH_2Cl_2 (6 cm^3) was added water (0.015 cm^3, 0.83 mmol). The progress of the hydrolysis reaction was monitored by ^{31}P-{^{1}H} NMR spectroscopy. In a separate experiment, water (0.015 cm^3, 0.83 mmol) was added to a pale yellow solution containing complex **10** (0.137 g, 0.168 mmol) and PPh_3 (0.045 g, 0.171 mmol) in CH_2Cl_2 (5 cm^3). The resultant mixture was monitored by ^{31}P-{^{1}H} NMR spectroscopy.

Crystallography

Intensity data for compounds **2** and **10** were collected on an Enraf-Nonius CAD-4 diffractometer at 294 K using graphite-monochromated Mo-Kα radiation (λ = 0.710 73 Å). Intensity data for **5** were collected on a Siemens P4 diffractometer at

Table 7 Atomic coordinates of complex **5**

Atom	*x*	*y*	*z*
Pt(1)	0.113 23(2)	0.181 72(3)	0.237 56(2)
Pt(2)	−0.056 58(2)	0.184 32(2)	0.122 85(2)
P(1)	0.118 5(1)	0.096 4(2)	0.369 7(2)
P(2)	0.014 4(1)	0.106 8(2)	0.114 3(2)
P(3)	0.075 2(1)	0.268 8(2)	0.168 1(2)
P(4)	0.157 0(1)	0.260 8(2)	0.313 8(2)
O(1)	0.152 9(3)	0.103 1(4)	0.311 5(4)
O(2)	0.069 6(3)	0.096 5(4)	0.178 2(4)
O(3)	0.005 7(3)	0.267 5(4)	0.125 9(4)
O(4)	0.125 4(3)	0.261 4(4)	0.374 1(4)
C(1)	0.069 7(5)	0.020 3(6)	0.356 2(7)
C(2)	−0.024 4(5)	0.023 0(5)	0.097 6(7)
C(3)	0.084 2(5)	0.347 8(6)	0.220 6(6)
C(4)	0.149 0(5)	0.345 0(6)	0.273 7(7)
C(11)	0.177 3(5)	0.076 8(6)	0.448 2(6)
C(12)	0.172 9(6)	0.098 8(7)	0.511 1(7)
C(13)	0.217 1(6)	0.079 9(8)	0.571 0(7)
C(14)	0.267 5(6)	0.038 7(7)	0.568 3(8)
C(15)	0.273 2(6)	0.018 1(7)	0.504 1(9)
C(16)	0.230 1(5)	0.036 3(7)	0.444 2(8)
C(21)	0.048 3(5)	0.123 8(6)	0.042 1(7)
C(22)	0.016 3(6)	0.160 4(7)	−0.015 1(8)
C(23)	0.042 4(8)	0.174 7(8)	−0.068 9(8)
C(24)	0.104 4(8)	0.150 6(8)	−0.063 9(9)
C(25)	0.135 4(7)	0.114 4(9)	−0.007 1(10)
C(26)	0.109 0(6)	0.101 8(6)	0.046 6(8)
C(31)	0.121 5(5)	0.289 1(6)	0.107 6(6)
C(32)	0.097 4(6)	0.333 2(7)	0.052 7(7)
C(33)	0.133 5(8)	0.350 9(7)	0.007 4(9)
C(34)	0.192 7(7)	0.330 3(8)	0.019 2(9)
C(35)	0.219 8(6)	0.285 4(8)	0.072 4(8)
C(36)	0.183 0(6)	0.264 6(7)	0.118 4(7)
C(41)	0.240 5(5)	0.247 1(6)	0.350 9(7)
C(42)	0.284 8(5)	0.260 1(7)	0.312 2(7)
C(43)	0.348 2(5)	0.250 9(7)	0.342 5(9)
C(45)	0.324 3(6)	0.214 5(7)	0.448 5(8)
C(46)	0.261 6(5)	0.226 0(6)	0.417 2(7)
C(44)	0.367 7(6)	0.226 2(7)	0.409 2(9)
C(1S)	0.073 2(7)	0.409 3(8)	0.422 0(9)
Cl(1)	0.053 9(2)	0.472 3(3)	0.359 1(3)
Cl(2)	0.060 2(2)	0.436 3(3)	0.500 5(3)
C(2S)	0.139 5(8)	−0.055 4(9)	0.228 8(9)
Cl(3)	0.199 5(2)	−0.087 0(3)	0.294 1(3)
Cl(4)	0.071 3(3)	−0.102 8(3)	0.218 1(3)
C(3S)	0.292 2(9)	0.080 0(10)	0.275 1(14)
Cl(5)	0.275 2(5)	0.097 6(6)	0.195 8(5)
Cl(6)	0.348 8(4)	0.020 4(4)	0.308 1(5)
C(4S)	0.0	0.345 6(39)	−0.25
Cl(7)	0.035 6(14)	0.329 7(9)	−0.185 1(10)

Table 8 Atomic coordinates of complex **10**

Atom	*x*	*y*	*z*
Pt(1)	0.104 55(3)	0.392 16(3)	0.293 42(2)
P(1)	0.184 9(2)	0.564 2(2)	0.393 4(2)
P(2)	0.198 6(2)	0.299 6(2)	0.402 2(2)
P(3)	0.045 6(2)	0.234 3(2)	0.174 7(2)
O(1)	0.092 2(6)	0.639 2(6)	0.409 4(5)
O(2)	0.101 6(6)	0.196 1(6)	0.462 7(5)
O(3)	0.062 2(7)	0.554 3(7)	0.155 7(6)
C(1)	0.225 5(9)	0.514 5(9)	0.505 0(6)
C(2)	0.294 9(9)	0.423 6(9)	0.487 0(7)
C(3)	0.010 5(9)	0.487 0(8)	0.212 4(7)
C(4)	−0.123 2(10)	0.464 6(10)	0.236 8(9)
C(11)	0.339 5(8)	0.674 4(8)	0.354 0(6)
C(12)	0.440 0(11)	0.745 2(11)	0.415 3(9)
C(13)	0.557 7(12)	0.823 1(13)	0.380 1(11)
C(14)	0.571 8(12)	0.829 2(14)	0.289 2(11)
C(15)	0.471 7(13)	0.761 0(12)	0.228 5(10)
C(16)	0.349 4(11)	0.686 1(11)	0.260 4(9)
C(21)	0.312 0(9)	0.228 6(10)	0.371 2(8)
C(22)	0.417 7(11)	0.302 5(15)	0.321 4(11)
C(23)	0.510 2(13)	0.248 4(21)	0.297 3(12)
C(24)	0.495 8(18)	0.126 7(20)	0.328 0(14)
C(25)	0.388 8(17)	0.060 3(16)	0.368 4(13)
C(26)	0.295 7(11)	0.109 0(11)	0.390 9(8)
C(31)	0.154 5(9)	0.283 1(11)	0.082 5(8)
C(32)	0.259 6(13)	0.394 6(19)	0.091 5(14)
C(33)	0.337 9(16)	0.443 2(19)	0.014 0(13)
C(34)	0.313 5(20)	0.361 1(21)	−0.064 7(14)
C(35)	0.205 7(16)	0.259 6(18)	−0.076 9(10)
C(36)	0.126 7(12)	0.220 8(13)	−0.005 6(9)
C(41)	0.047 3(10)	0.080 0(9)	0.208 1(7)
C(42)	0.124 3(12)	0.027 4(12)	0.165 1(9)
C(43)	0.125 1(18)	0.088 6(14)	0.191 9(12)
C(44)	0.052 8(19)	−0.148 2(14)	0.260 7(14)
C(45)	−0.026 0(14)	−0.096 1(11)	0.308 8(10)
C(46)	−0.027 6(10)	0.019 2(9)	0.279 0(8)
C(51)	−0.113 7(8)	0.202 6(8)	0.116 2(6)
C(52)	−0.125 7(10)	0.277 5(10)	0.043 2(8)
C(53)	−0.246 4(11)	0.258 7(12)	0.004 4(8)
C(54)	−0.357 6(11)	0.170 4(14)	0.034 3(10)
C(55)	−0.347 4(11)	0.094 9(14)	0.108 0(10)
C(56)	−0.226 5(12)	0.113 5(13)	0.144 5(9)
Cl(1)	−0.174 1(3)	0.177 6(3)	0.432 1(2)

210 K using the same radiation. The ω-scan technique was applied with variable scan speeds. Intensities of three standard reflections measured every 2 h, for each crystal, showed negligible variation. For all compounds the heavy-atom positions were solved by Patterson methods and the locations of all non-hydrogen atoms were determined from subsequent Fourier-difference syntheses. In each case all non-hydrogen atoms were refined with anisotropic thermal parameters by full-matrix least squares to minimize $\Sigma w(F_o - F_c)^2$, where $w^{-1} = \sigma^2(F_o) + gF_o^2$. Hydrogen atoms bonded to carbon atoms were positioned on geometric grounds (C–H 0.96 Å) and included in the refinement as riding atoms with general thermal parameters for each structure. The hydrogen atoms bonded to oxygen in structures **2** and **10** were refined with isotropic thermal parameters. Crystal data, data collection, and least-squares parameters are listed in Table 5.

All calculations were performed using SHELXTL-PC[9] on a 486-66 personal computer. Atomic coordinates are in Tables 6–8.

Complete atomic coordinates, thermal parameters and bond lengths and angles have been deposited at the Cambridge Crystallographic Data Centre. See Instructions for Authors, *J. Chem. Soc., Dalton Trans.*, 1996, Issue 1.

Acknowledgements

We thank the Natural Sciences and Engineering Research Council of Cananda for financial support.

References

1 D. M. Roundhill, R. P. Sperline and W. B. Beaulieu, *Coord. Chem. Rev.*, 1978, **26**, 263.
2 H. Goldwhite, *Introduction to Phosphorus Chemistry*, Cambridge University Press, Cambridge, 1981, pp. 306–308.
3 V. I. Nefedov, Y. V. Salyn, B. Walther, B. Messbauer and R. Schops, *Inorg. Chim. Acta*, 1980, **45**, L103.
4 J. Powell, M. J. Horvath and A. Lough, *J. Chem. Soc., Dalton Trans.*, 1995, 2975.

5 T. G. Appleton, M. A. Bennet and I. B. Tomkins, *J. Chem. Soc., Dalton Trans.*, 1976, 439; T. G. Appleton, H. C. Clark and L. E. Manzer, *Coord. Chem. Rev.*, 1973, **10**, 335.

6 M. N. S. Hill, B. F. G. Johnson and J. Lewis, *J. Chem. Soc. A*, 1971, 2341.

7 N. W. Alcock, P. Bergamini, T. M. Gomes-Carniero, R. D. Jackson, J. Nicholls, A. G. Orpen, P. G. Pringle, S. Sostero and O. Traverso, *J. Chem. Soc., Chem. Commun.*, 1990, 980.

8 J. X. McDermott, J. F. White and G. M. Whitesides, *J. Am. Chem. Soc.*, 1976, **98**, 6521.

9 G. M. Sheldrick, SHELXTL-PC, Siemens Analytical X-Ray Instruments Inc., Madison, WI, 1990.

Received 12*th September* 1995; *Paper* 5/06025G